



OPEN

Anti-CD321 antibody immunotherapy protects liver against ischemia and reperfusion-induced injury

Enzhi Yin¹, Takeshi Fukuhara²✉, Kazuyoshi Takeda^{3,4}, Yuko Kojima⁵, Kyoko Fukuhara⁶, Kenichi Ikejima⁶, Hisashi Bashuda¹, Jiro Kitaura¹, Hideo Yagita⁷, Ko Okumura^{1,4} & Koichiro Uchida⁸✉

The prognosis of the liver transplant patients was frequently deteriorated by ischemia and reperfusion injury (IRI) in the liver. Infiltration of inflammatory cells is reported to play critical roles in the pathogenesis of hepatic IRI. Although T lymphocytes, neutrophils and monocytes infiltrated into the liver underwent IRI, we found that neutrophil depletion significantly attenuated the injury and serum liver enzyme levels in a murine model. Interestingly, the expression of CD321/JAM-A/F11R, one of essential molecules for transmigration of circulating leukocytes into inflammatory tissues, was significantly augmented on hepatic sinusoid endothelium at 1 h after ischemia and maintained until 45 min after reperfusion. The intraportal administration of anti-CD321 monoclonal antibody (90G4) significantly inhibited the leukocytes infiltration after reperfusion and diminished the damage responses by hepatic IRI (serum liver enzymes, inflammatory cytokines and hepatocyte cell death). Taken together, presented results demonstrated that blockade of CD321 by 90G4 antibody significantly attenuated hepatic IRI accompanied with substantial inhibition of leukocytes infiltration, particularly inhibition of neutrophil infiltration in the early phase of reperfusion. Thus, our work offers a potent therapeutic target, CD321, for preventing liver IRI.

Ischemia and reperfusion injury (IRI) in the liver is an inevitable consequence of a number of common clinical situations and operative procedures that include circulatory shock, stroke, myocardial infarction and hepatectomy¹. Especially in liver transplantation, IRI is recognized as the critical event to modulate prognosis of the patients². Nevertheless, there is no practical and effective therapy to avoid hepatic IRI except for ischemic preconditioning³. Thus, it is important to reveal the mechanisms of hepatic IRI, particularly in reperfusion phase, for developing novel therapeutic strategies⁴.

It has been shown that the pathophysiological process of IRI is consisted with two phases, ischemia phase followed by reperfusion phase⁵. Ischemia potentiates oxidative-stress mediated tissue damage due to the reentry of oxygenated blood^{6,7}. Reactive oxygen species (ROS) activate Kupffer cells in concomitant with producing inflammatory cytokines, chemokines and other mediators. Sequentially in reperfusion phase, an acute inflammatory response will be triggered by chemoattraction and activation of leukocytes, resulting in massive tissue damage^{8,9}.

During these processes, it has to be evaluated whether trans-endothelial migration (TEM) of leukocytes is a key mechanism in prognosis as well as a therapeutic target in hepatic IRI. Inflammatory leukocytes undergo multiple and sequential steps under the strict control by coordinated surface molecules, then there are several reports showing the antibodies to block TEM¹⁰. Among the molecules on vascular surface, CD321 (a.k.a. Junctional

¹Atopy Research Center, Juntendo University Graduate School of Medicine, Tokyo, Japan. ²Department of Neurology, Juntendo University Graduate School of Medicine, 2-1-1 Hongo, Bunkyo-ku, Tokyo 113-8421, Japan. ³Laboratory of Cell Biology, Research Support Center, Juntendo University Graduate School of Medicine, Tokyo, Japan. ⁴Department of Biofunctional Microbiota, Juntendo University Graduate School of Medicine, Tokyo, Japan. ⁵Laboratory of Morphology and Image Analysis, Research Support Center, Juntendo University Graduate School of Medicine, Tokyo, Japan. ⁶Department of Gastroenterology, Juntendo University Graduate School of Medicine, Tokyo, Japan. ⁷Department of Immunology, Juntendo University School of Medicine, Tokyo, Japan. ⁸Juntendo Advanced Research Institute for Health Science, Juntendo University School of Medicine, 2-1-1 Hongo, Bunkyo-ku, Tokyo 113-8421, Japan. ✉email: noantibody-noscience@umin.ac.jp; k-uchida@umin.ac.jp

Adhesion Molecule A or F11R) has been characterized as one of the essential molecules for TEM at the site of inflammation¹⁰. CD321 localizes at intercellular tight junction of endothelial cells to support barrier function under physiological conditions, but ischemia or inflammation stimulates subcellular relocalization as well as diapedesis of lymphocyte via LFA-1 binding^{11,12}. Hepatic IRI was exaggerated in constitutive CD321-deficient mice despite reduction of neutrophil transmigration¹³. These results suggested hepatic IRI is regulated differently in multiple steps by CD321. Although the role of CD321 in the infiltration of neutrophil or homeostatic recovery of barrier function after hepatic IRI is unclear, it has been shown that inhibition of CD321 protein with anti-CD321 monoclonal antibody (mAb) (clone BV11) blocked neutrophil recruitment in experimental meningitis model¹⁴. Then, we here examined the therapeutic efficiency of anti-CD321 mAb (90G4) treatment in hepatic IRI model.

Results

Neutrophil depletion inhibited liver damage in a murine hepatic IRI model. We have established the experimental mice hepatic IRI model that induce massive cell death in the liver (Fig. 1A,B). Infiltrated population of T lymphocytes, neutrophils, monocytes were quantified at several time points after reperfusion. The results showed that neutrophils are substantially major rather than other leukocytes (Fig. 1C). To examine the role of neutrophil for hepatic IRI, we treated the mice with anti-Gr-1 mAb to deplete neutrophils at 6 and 4 days prior to liver surgery¹⁵. Flow cytometric analysis confirmed that anti-Gr-1 mAb treatment effectively depleted neutrophils, but not monocytes in peripheral blood mononuclear cells (PBMCs) (Fig. 1D). In this neutrophil-depletion model, the results provided efficient protection with significant reduction in both serum glutamic oxaloacetic transaminase (GOT) and glutamic pyruvic transaminase (GPT) levels (Fig. 1E). These results confirmed that neutrophils play a critical role for hepatic IRI.

Transient upregulation of CD321 upon hepatic IRI. Expression of CD321 is characterized in various cell types in tissues including the vasculature under physiological and disease conditions, and CD321 has been reported to play critical roles for neutrophil infiltration into the ischemic region^{13,16}. Immunohistochemical staining using 90G4 antibody demonstrated increased CD321 expression on hepatic sinusoid endothelium 2 and 6 h after reperfusion in the hepatic IRI model. There was no staining in the sham-operated mice by immunohistochemical analysis (Fig. 2A). This finding was further confirmed by the quantitative polymerase chain reaction (qPCR) analysis, demonstrating that CD321 expression was immediately upregulated in response to ischemia (0 min) with sustained expression during reperfusion phase until 60 min, when compared with the sham-operated mice (Fig. 2B).

Moreover, we examined the expression level of lymphocyte function-associated antigen 1 (LFA-1 known as CD11a/CD18 or α L β 2) known as a primary ligand of vascular CD321 for diapedesis of leukocytes into inflammatory sites^{10,11,17}. In damaged liver at 2 h after reperfusion, the results clearly showed that LFA-1 was expressed on T lymphocytes, neutrophils and monocytes (Fig. 2C). These results suggest that CD321 might play a role to regulate the infiltration of inflammatory cells in an early-phase of hepatic IRI.

Anti-CD321 mAb treatment inhibited leukocyte infiltration into the liver after IRI. Given the evidence of CD321 upregulation in ischemic liver, we hypothesized that LFA-1 positive lymphocytes infiltrate via LFA-1/CD321 molecular interaction. To inhibit trans-endothelial migration and subsequent liver IRI, we evaluated the therapeutic efficacy of anti-CD321 mAb (90G4). The antibody was administrated through the portal vein after the removal of the micro-clip for reperfusion, subsequently, the infiltrating non-parenchymal cells in the livers were quantified. The treatment with 90G4 mAb reduced the number of non-parenchymal cells significantly at 2 h, but not 6 h after reperfusion compared with IgG-treated mice (Fig. 3A). At 2 h after reperfusion, we found that the infiltration of CD45⁺ cell population, including neutrophils, T cells and monocytes, appeared to be decreased in number by 90G4 antibody administration. When this result was expressed as percentage of CD45⁺ cells, the infiltration of neutrophil, but not T cell or monocyte, was significantly decreased (Fig. 3B). The liver sections were subjected for immunohistochemical staining with anti-Ly6G antibody which specifically detect neutrophil, resulting in confirmation of dramatic reduction of infiltrated neutrophil in 90G4 antibody treated group (Fig. 3C). At 6 h after reperfusion, 90G4 treatment did not alter the percentage or quantity of T cells and neutrophils in the ischemic lobes, nevertheless, mice treated with 90G4 mAb had a lower percentage and number of monocytes with statistically significance (Fig. S1). Thus, 90G4 mAb inhibited the interaction between neutrophilic LFA-1 and vascular CD321 at an early phase after reperfusion, implying for the therapeutic potency of CD321 blockade.

Anti-CD321 mAb treatment attenuated hepatic IRI. We revealed that neutrophil depletion by Gr-1 mAb treatment is necessary for the protection of hepatic IRI. Because vascular CD321 was rapidly upregulated in liver upon ischemia, blocking LFA-1/CD321 is a potent target of therapeutics for hepatic protection. In fact, inhibition of CD321 by 90G4 mAb suspended neutrophil infiltration at an early phase after hepatic IRI. We next examined whether 90G4 mAb is sufficient for the protection of hepatic IRI. The result showed that 90G4 mAb treatment significantly reduced serum GOT and GPT levels from 2 to 24 h after reperfusion compared with the IgG-treated mice (Fig. 4A). Suzuki score¹⁸ demonstrated that necrotic regions were significantly reduced in the liver of 90G4-treated mice (Fig. 4B,C). Consistently, the protected liver showed the reduced number of Caspase-3 positive cells as well as terminal deoxynucleotidyl transferase-mediated deoxyuridine triphosphate nick end labeling (TUNEL) positive cells (Fig. 4D–F).

As the detail mechanism of hepatic protection by 90G4 mAb treatment, we examined serum level of interleukin (IL) -6 or tumor necrosis factor (TNF) - α , inflammatory cytokines reported to play a key role to activate infiltrating leukocytes in the inflamed liver^{19,20}. 90G4 mAb treatment significantly lowered serum IL-6 level at 2 and 6 h after reperfusion and serum TNF- α level at 2 h after reperfusion respectively (Fig. 4G). In summary, these

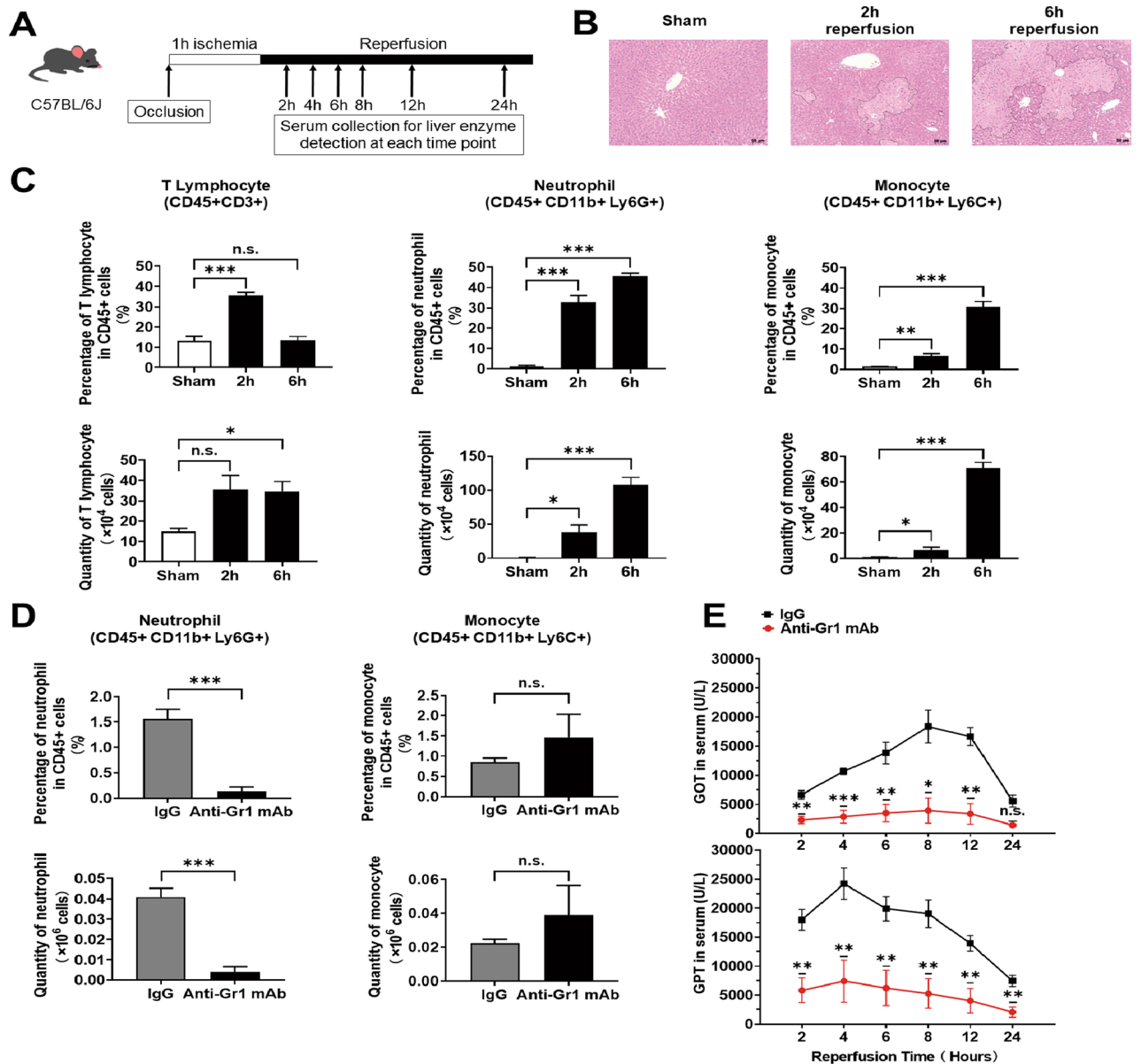


Figure 1. Hepatic IRI was alleviated by neutrophil depletion. (A) Protocol for a murine hepatic IRI model. (B) Representative images of hematoxylin and eosin staining of ischemic liver at indicated time after reperfusion. Necrosis areas are surrounded by dashed line. Image of the liver of the sham-operated mice were not distinguishable between 2 and 6 h after the sham-operation, thus the image of the liver at 6 h after sham-operation is demonstrated. (C) Percentage and the number of intrahepatic infiltrating T lymphocytes, neutrophil and monocyte in ischemic livers at 2 h and 6 h after reperfusion (n = 3–5 in each group). (D) Mice were treated with anti-Gr1 mAb at 6 and 4 days before the experiments, and PBMCs were obtained promptly before the experiments to confirm neutrophil depletion. Percentage and number of neutrophils and monocytes in PBMCs of anti-Gr1 mAb-treated and control (rat IgG2b)-treated mice are presented (n = 3 in each group). (E) Sera were collected at the indicated time after reperfusion from the hepatic IRI mice treated with anti-Gr1 mAb or control rat IgG2b. Then, serum GOT and GPT levels were examined. n = 3 mice in each group. *P < 0.05, **P < 0.01, ***P < 0.001. n.s. not significant. Results are presented as Means \pm standard error of the mean (SEM) (C to E). Data derived from at least N = 2 independent experiments.

results presented that 90G4 administration ameliorated hepatic IRI by inhibiting the infiltration of neutrophil, which is a major producer of inflammatory cytokines.

Discussion

Although IRI is induced by both oxidative stress after blood resupply, irreversible damage of hepatocyte is caused mainly by inflammatory leukocytes migrating into the liver²¹. However, current therapeutic approaches are limited and unsatisfactory. Here, we demonstrated that infiltrating neutrophils played an essential role in

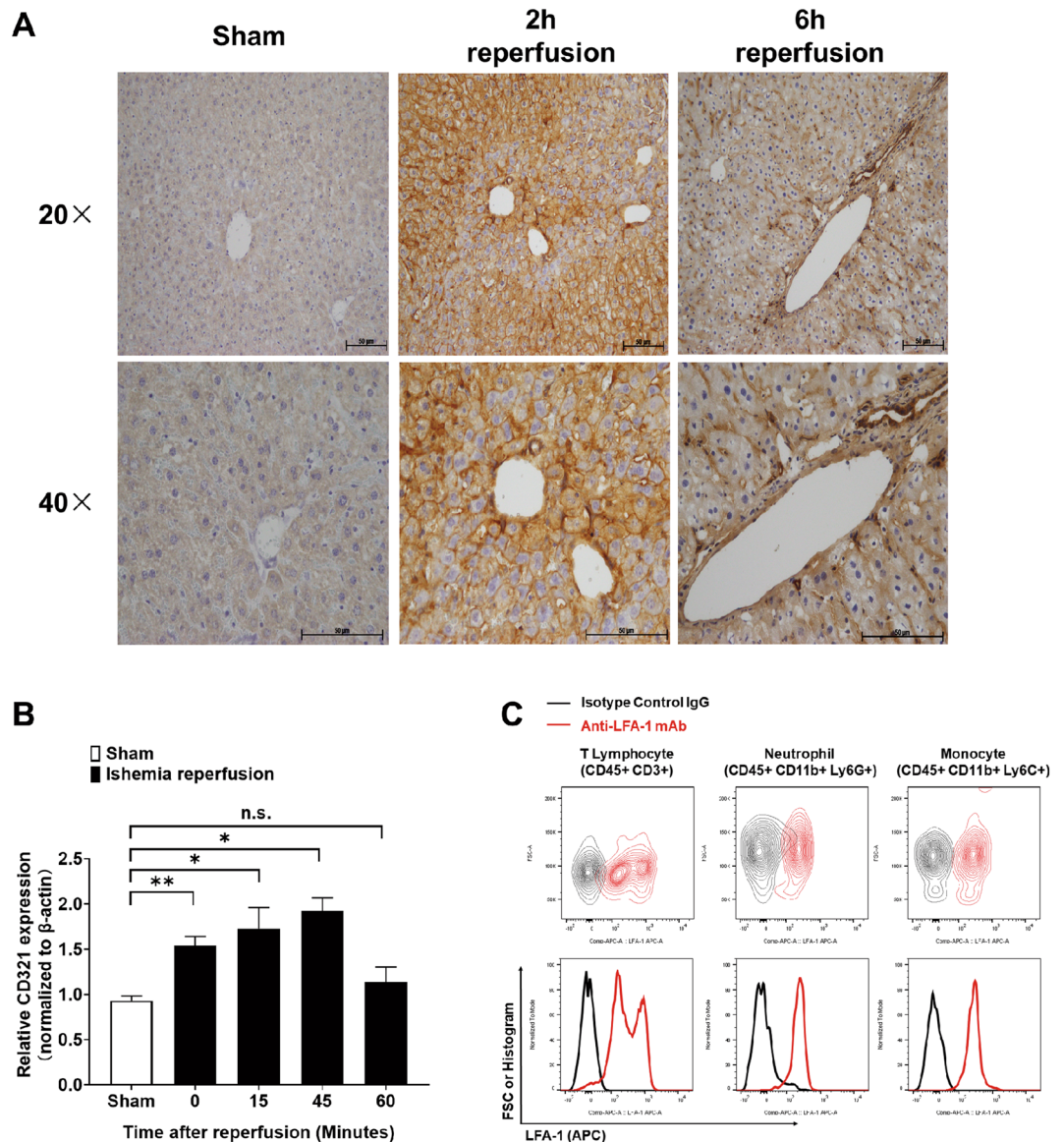


Figure 2. Transient CD321 expression in liver underwent IRI. **(A)** Representative immunohistochemical staining images for CD321 (dark brown staining) in damaged liver. Livers were extracted from the sham-operated mice and the IRI mice at 2 and 6 h after reperfusion. Magnification, $\times 20$ and $\times 40$. Image of the liver of the sham-operated mice were not distinguishable between 2 and 6 h after the sham-operation, thus the image of the liver at 6 h after the sham-operation is demonstrated. **(B)** Relative CD321 mRNA expression levels in livers. mRNAs were obtained from the ischemic lobes at the indicated time after reperfusion and from the sham-operated liver at 30 min after sham-operation. $n = 3$ in each group. $*P < 0.05$, $**P < 0.01$. n.s., not significant. Results are presented as Means \pm SEM. **(C)** Representative expression profile of LFA-1 (ligand of CD321) on indicated leukocytes infiltrating in liver after IRI. $n = 3$ in each group. Infiltrating leukocytes were prepared from liver at 2 h after reperfusion, then LFA-1 expression of the indicated leukocytes population was examined by flow cytometry as described in methods. Data derived from $N = 2$ experiments.

triggering hepatic IRI. CD321 immunotherapy using 90G4 antibody provided dramatic suppression of hepatic IRI via decreased number of leukocytes, especially in the early phase after reperfusion.

It has been shown that hepatic IRI composed of two distinct phases of innate immune responses²². The initial phase (< 2 h after reperfusion) involves Kupffer cell activation to produce free radicals, cytokines, and chemokines²⁰. In the late phase, the produced cytokines activate infiltrated leukocytes, leading to the irreversible damage of hepatocytes. Kupffer cells are characterized as the main source of primary inflammatory mediator, such as $\text{TNF-}\alpha$ ^{23,24}, in hepatic IRI. As an alternative role of $\text{TNF-}\alpha$, it has been shown that $\text{TNF-}\alpha$ stimulates to induce CD321 redistribution on endothelial cells, assisting neutrophil transmigration to the inflamed tissue²⁵. In the late phase, neutrophils also produce $\text{TNF-}\alpha$ ²⁶, but a central role of $\text{TNF-}\alpha$ is to induce simultaneous inflammation like IL-6 production mediated by monocytes and endothelial cells²⁷, leading to exaggerate the

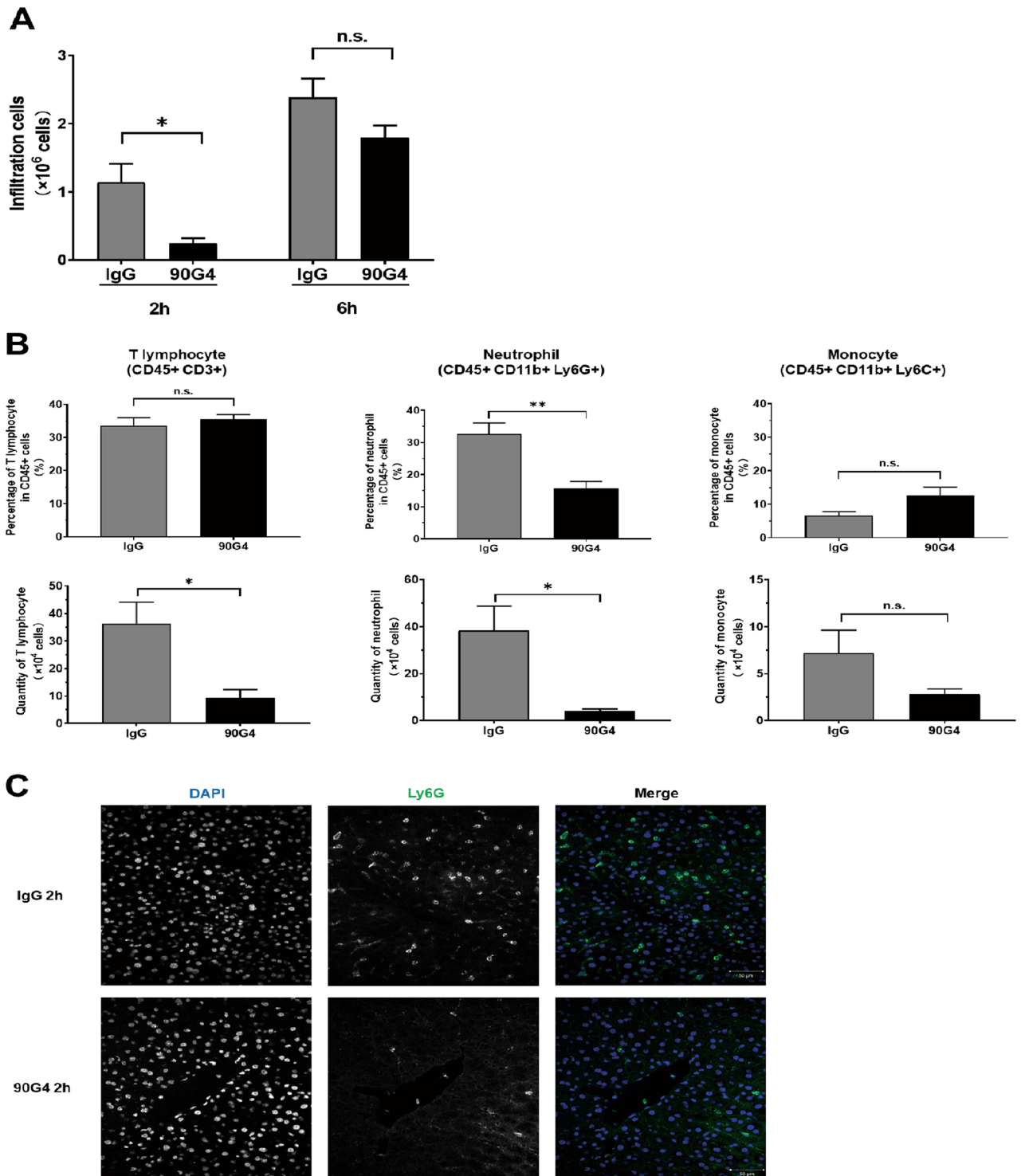


Figure 3. Anti-CD321 mAb (90G4) inhibited leukocyte infiltration in liver after IRI. (A) Quantity of nonparenchymal cells in liver suffered IRI. Nonparenchymal cells were prepared from ischemic liver of the mice treated with indicated mAb at 2 h and 6 h after reperfusion. (B) Percentage and quantity of intrahepatic infiltrating T lymphocytes, neutrophils and monocytes from the mice treated with indicated mAb at 2 h after reperfusion. (C) Representative images of immunocytochemical analysis of Ly6G positive cells, neutrophil, in ischemic liver at 2 h after reperfusion. Cryosections were stained with DAPI (blue) and anti-Ly6G antibody (green). Scale bar, 50 μ m. Magnification, \times 40. $n = 5$ in each group. * $P < 0.05$, ** $P < 0.01$. *n.s.* not significant. Results are presented as Means \pm SEM.

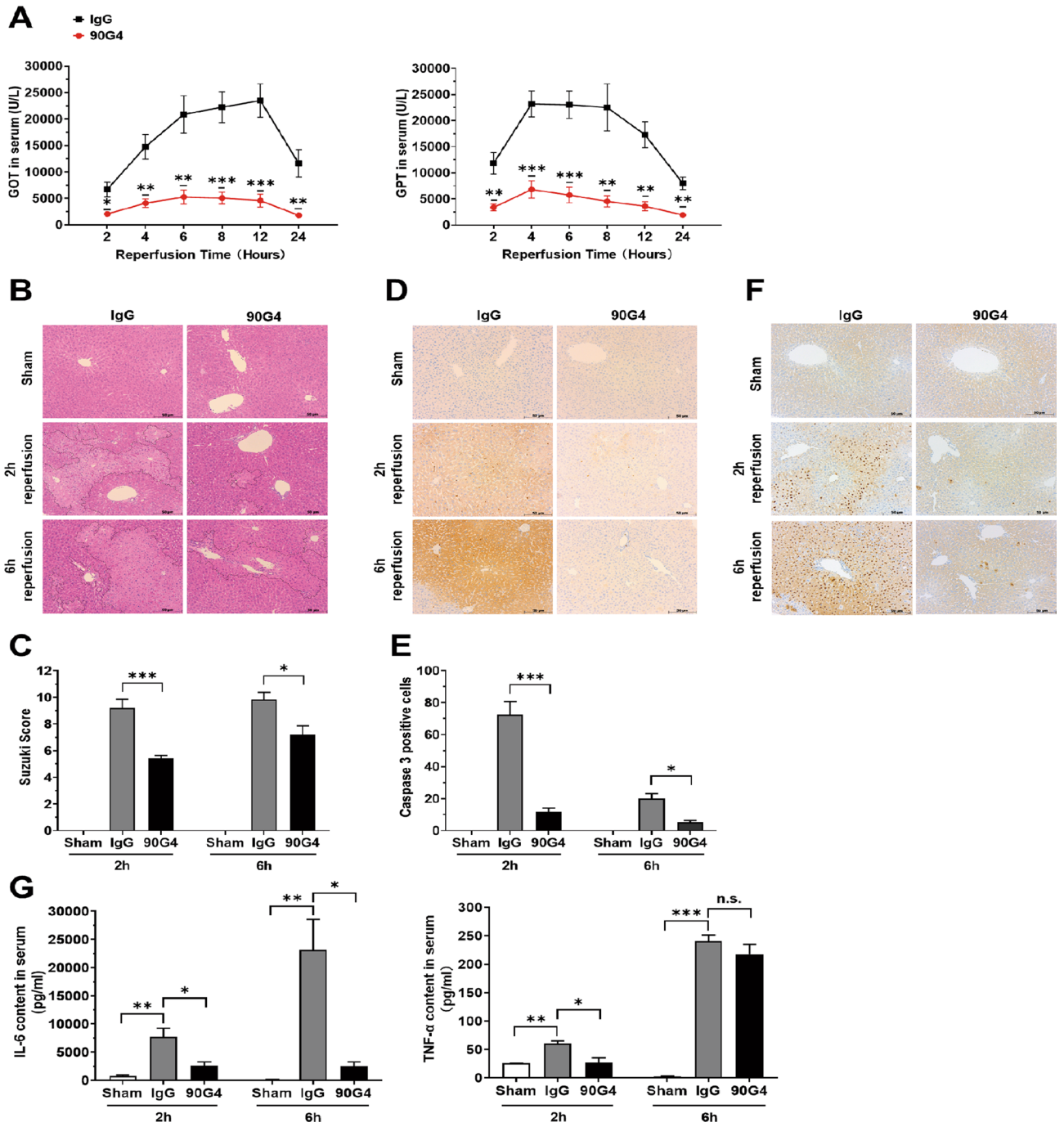


Figure 4. Anti-CD321 mAb (90G4) treatment inhibits hepatic IRI. (A) Serum GOT and GPT levels in 90G4-treated hepatic IRI mice. Sera were collected at the indicated time after the reperfusion from the hepatic IRI mice treated with 90G4 or rat IgG, then serum GOT and GPT levels were examined (n = 5–7 in each group). (B) Representative images of hematoxylin and eosin staining of damaged livers from indicated antibody-treated mice at indicated times after reperfusion. Necrotic areas are surrounded by dashed lines. (C) Histologic injury score of hematoxylin and eosin staining sections analyzed by Suzuki criteria (n = 3 mice in sham group and n = 5–6 mice in IRI group). (D) Representative images of Caspase-3 staining of livers at the indicated time after reperfusion of the indicated antibody-treated mice. (E) Caspase-3 positive cells (dark brown spots in Figure D) were counted and analyzed using Image J software (n = 3 mice in sham group and n = 5–6 mice in IRI group). (F) Representative images of TUNEL staining of ischemic livers at the indicated time after the reperfusion of the indicated antibody-treated mice (n = 3 in each group). (G) Serum IL-6 and TNF-α levels. Serum was collected from the sham-operated mice and IRI mice treated with indicated mAb at 2 and 6 h after the reperfusion. The amount of IL-6 and TNF-α was measured by ELISA (n = 3 mice in sham group and 5–6 mice in IRI group). *P < 0.05, **P < 0.01, ***P < 0.001. Results are presented as Mean ± SEM (C,E,G). Magnification, × 20 (B,D,F). N = 2–3 independent experiments.

liver injury further²⁸. Thus, 90G4 mAb mediated-inhibition of neutrophil infiltration at early phase would be extremely beneficial for subsequent suppression of TNF- α production in the late phase to cause hepatic damage.

It has been considered that leukocytes infiltration are regulated in organ-specific and cell-type specific mechanism²⁹, but this is because the multi-steps in diapedesis are under the strict control by multiple surface molecules. For example, CD321 plays an essential role for transmigration at the final step of diapedesis into inflammatory tissues underwent heart IRI model¹². Similarly, our presented results in hepatic IRI model demonstrated that CD321 blockade inhibited neutrophil infiltration and hepatic injury. 90G4 mAb treatment suspended all the injury markers: necrosis and apoptosis of hepatocytes, secretion of GOT and GPT, upregulation of TNF- α and IL-6.

Previous experiments utilizing CD321-deficient mice demonstrated that apoptotic hepatocytes were increased despite the suppression of neutrophil infiltration upon hepatic IRI. In this case, serum GOT and GPT levels were not changed¹³. We firstly need to understand that the inhibition of CD321 function by either knockout animal or blocking antibody provide a different situation in terms of mechanism. Notably, presented results demonstrated that inhibition of neutrophil infiltration at an early phase sufficiently reduced hepatic IRI. Thus, transient inhibition of CD321 by 90G4 mAb might have advantage to inhibit hepatic injury in our IRI model. Since 90G4 mAb reacts in-situ in the context of pathophysiological processes unlike constitutive knockout, it reminds that CD321 is the bona fide therapeutic target in hepatic IRI. Further studies are required to reveal the mechanisms of monocyte infiltration upon hepatic IRI and the role of infiltrating monocytes for hepatic IRI. Besides, it also has to be considered the underlying mechanism by junctional adhesion molecule (JAM) family members for regulating tight junction. Given the evidence that JAM-C plays a crucial role on tissue repairing, the interplay of CD321 with other JAM family member could be important especially at the resolution phase (several days after reperfusion)^{30,31}.

CD321 is redistributed and internalized in endothelial cells upon hypoxic stimulation or inflammatory stimulation^{32,33}. As a therapeutic target, dual roles of CD321 for tight junction formation and lymphocyte diapedesis upon stimuli provide potent characters in inflammation-dependent accessibility of immunotherapeutics. In fact, CD321 is a proven therapeutic target of peritonitis, skin inflammation, meningitis, and heart IRI^{11,34–36}. In summary, our findings propose that disrupting human LFA-1/CD321 interaction is the useful and attractive strategy to inhibit trans-endothelial migration of neutrophils for protecting hepatic IRI in clinic.

Methods

Study design. The aim of this study is to investigate the effect of intraportal administration of anti-CD321 monoclonal antibody (90G4) with regard to liver IRI in a murine model. Group size was determined by power analysis using the effect size from pilot experiments. All mice in this study were randomized before treatment. To ascertain the mechanism of acute phase in hepatic IRI, we set end points at 24 h after reperfusion in vivo study. By taking careful consideration of abnormal anatomy of mice, mice that failed to establish at least 70% of damage after liver IR due to anatomically abnormal structure were excluded from the analysis (Fig. S2). The researchers were blinded to conduct of the experiment and assessment of outcomes.

Reagents. Rat anti-mouse CD321 mAb, clone 90G4³², and anti-Gr-1 mAb, clone RB6-8C5³⁷, were prepared and purified in our laboratory as previously described. As a control antibody, rat IgG was purchased from Southern Biotech (Birmingham, AL, USA). All antibodies used in this study was dialyzed in 0.9% NaCl prior to injection.

Animal liver IRI model. Four- to six-week-old wildtype male C57BL/6J mice were purchased from Charles River Japan Inc. (Yokohama, Japan) and maintained in the specific pathogen-free facility at Juntendo University. Eight- to ten-week-old mice were subjected to establish a warm 70% liver IRI model as described in the literature^{3,38–42} (Fig. 1A). Briefly, mice were anesthetized through intraperitoneal injection with pentobarbital sodium. A micro-clamp was placed at porta hepatis right above the branching to the right lateral lobe to interrupt the blood flow for 1 h. Mice body temperature was maintained at 37 °C on a heating plate. Either 90G4 antibody or rat IgG (300 μ g per mouse) was injected through the portal vein promptly after removing the micro-clamp. All the same procedure but flow occlusion was performed in the mice of sham group. All protocol was approved by Medicine Animal Ethics Committee of Juntendo University (Approved number 2020131). All animal experiments were performed in compliance with the applicable national laws and regulations, the institutional guidelines and ARRIVE guidelines on animal experimentation. All the experimental protocols involving animals are reviewed by the institutional animal care and use committee.

Histopathology and immunohistochemical analysis. Ischemic liver lobes were harvested and snap frozen in liquid nitrogen at 2 and 6 h after reperfusion. Liver sections with 6 μ m of thickness were fixed with 4% paraformaldehyde in phosphate buffer solution, in the following treatment with 0.3% hydrogen peroxidase to inhibit endogenous peroxidase activity. Sections were incubated with rat anti-mouse 90G4 antibody (2 μ g per section) as primary antibody overnight, and biotin-streptavidin donkey anti-rat IgG (H + L) (1 μ g per section) as secondary antibody for 2 h. Then, samples were incubated with pre-formed streptavidin/biotin complex (ABC kit, Nacalai Tesque, Kyoto, Japan), and subsequent colorimetric development with diaminobenzidine substrates as the manual instructed (DAB kit, Nacalai Tesque, Kyoto, Japan).

Hematoxylin and eosin (H&E) staining was performed as described previously⁴³. Stained sections were analyzed in a double-blinded manner. A Suzuki score was calculated based on evaluation of congestion, vacuolization, and necrosis¹⁸. In the immunohistochemical evaluation of apoptotic cell death, tissue sections were stained with rabbit anti-cleaved caspase-3 (Asp175) (Cell Signaling Technology, Denver, MA, USA) as described

previously⁴⁴. TUNEL staining was employed for paraffin-embedded liver sections as described previously⁴⁵. Cryosections of the ischemic liver at 2 h reperfusion were stained with anti-mouse Ly6G (Clone 1A8) (Biolegend, San Diego CA, USA), which was followed by staining with Alexa Fluor 488-conjugated anti-rat IgG (H + L) (Invitrogen). Sections were counterstained with DAPI (Invitrogen)⁴⁶. Images were captured by AxioVision software of Zeiss Axio Lab.A1 microscope with attached AxioCam ERc 5S. Fluorescent images were obtained and analyzed using a FV300 confocal laser microscopy (Fluoview laser scanning biological microscope JX70 system; Olympus, Albertslund, Denmark).

Analysis of CD321 transcript by qPCR. After one hour of blood flow occlusion, the treated livers were harvested at each time point (15, 45 and 60 min) after reperfusion, and immediately fixed in TRI Reagent (TRI118, Cosmo Bio, Tokyo, Japan). Total RNA was isolated from the tissues by RNeasy Mini kit (Qiagen, Tokyo, Japan), then total RNA (0.1 µg per sample) was subjected to reverse transcription to cDNA in 8 µl of reaction volume using a qPCR kit (Toyobo, Osaka, Japan) according to the instruction manual. Real-time qPCR was performed for CD321 gene (Mm00554113_m1) and β-actin (Mm00607939_s1) with a TaqMan Universal PCR Master Mix on the StepOnePlus System (Applied Biosystems of Thermo Fisher Scientific, Waltham, Mass, USA). Quantitative level of CD321 mRNA transcript was normalized to mouse β-actin mRNA expression by a comparative C_T method.

Quantification of injury level by measurement of serum liver enzymes. Peripheral blood (P.B.) samples were collected via tail at 2, 4, 6, 8, 12 and 24 h after reperfusion, and centrifuged at 1300×g for 20 min. Serum samples were retrieved and stored in a – 80 °C deep freezer until measurement. Levels of GOT and GPT were measured by using a dri-chem slide kit on a Multi-purpose automatic dry-chemistry analyzer (Fujifilm, Tokyo, Japan).

Flow cytometry analysis. Non-parenchymal cells were isolated from liver as previously described⁴⁷. Briefly, after perfusion with 30 ml of phosphate-buffered saline (PBS), liver was grinded on a stainless-steel mesh and suspended in PBS containing 3% fetal bovine serum. After single centrifugation at 820×g for 10 min, pellet was suspended in the 30% Percoll for further separation with centrifugation at 660×g for 18 min at room temperature without brakes. The pellet was resuspended in red blood cell-lysis buffer for hemolysis, then washed once in PBS containing 3% fetal bovine serum. For staining, cells were incubated with viability dye and fluorochrome-conjugated antibodies: Zombie dye (Zombie Violet Fixable Viability Kit), CD45.2 (PerCP; clone 104), CD3 (PE/Cy7 or PE; clone 17A2), CD11b (Violet 421 or PE; clone M1/70), Ly6G (APC or APC/Cy7; clone 1A8), Ly6C (PE or FITC; clone HK1.4), F4/80 (FITC; clone BM8), and LFA-1 (APC; clone H155-78). All reagents were purchased from BioLegend (Biolegend, San Diego, CA, USA). Flow cytometry analysis was performed by BD FACSVerser, and data were analyzed with FlowJo software (BD Biosciences, San Jose, CA, USA). For identifying specific cell types, gating strategy was subjected to define T lymphocyte (CD45⁺CD3⁺), neutrophil (CD45⁺CD11b⁺Ly6G⁺), and monocyte (CD45⁺CD11b⁺Ly6C⁺) respectively.

Enzyme linked immunosorbent assay (ELISA). Serum samples were collected at 2 and 6 h after liver IRI. The concentration of IL-6 or TNF-α in serum was detected separately by corresponding Quantikine ELISA kit (R&D Systems, Minneapolis, MN, USA) following the manufacturer's instructions.

Neutrophil depletion. Circulating neutrophil was depleted via intraperitoneal injections of anti Gr-1 mAb (100 µg per mouse) on the day 0 and 2, which are corresponding to 6 and 4 days prior to induce ischemia¹⁵. The quantity of neutrophil and monocyte in P.B. were analyzed by flow cytometry to confirm the accomplishment of depletion on the day 6 after the first injection.

Statistical analysis. Obtained data were visualized by Prism software in graph with means ± SEM. Statistical differences between two groups were assessed by an unpaired Student's *t* test. *P* value of less than 0.05 was regarded as statistically significant.

Received: 24 July 2020; Accepted: 23 February 2021

Published online: 18 March 2021

References

1. Bosch, J. & Forns, X. Therapy. Statins and liver disease: from concern to “wonder” drugs?. *Nat. Rev. Gastroenterol. Hepatol.* **12**, 320–321. <https://doi.org/10.1038/nrgastro.2015.78> (2015).
2. Zhai, Y., Petrowsky, H., Hong, J. C., Busuttill, R. W. & Kupiec-Weglinski, J. W. Ischaemia-reperfusion injury in liver transplantation—from bench to bedside. *Nat. Rev. Gastroenterol. Hepatol.* **10**, 79–89. <https://doi.org/10.1038/nrgastro.2012.225> (2013).
3. Zhang, X. J. *et al.* An ALOX12-12-HETE-GPR31 signaling axis is a key mediator of hepatic ischemia-reperfusion injury. *Nat. Med.* **24**, 73–83. <https://doi.org/10.1038/nm.4451> (2018).
4. Dickson, I. Improving hepatic ischaemia-reperfusion injury outcomes. *Nat. Rev. Gastroenterol. Hepatol.* **16**, 583. <https://doi.org/10.1038/s41575-019-0194-y> (2019).
5. Lu, L. *et al.* Innate immune regulations and liver ischemia-reperfusion injury. *Transplantation* **100**, 2601–2610. <https://doi.org/10.1097/TP.0000000000001411> (2016).
6. Garcia-Prieto, J. *et al.* Neutrophil stunning by metoprolol reduces infarct size. *Nat. Commun.* **8**, 14780. <https://doi.org/10.1038/ncomms14780> (2017).

7. Eltzschig, H. K. & Eckle, T. Ischemia and reperfusion—from mechanism to translation. *Nat. Med.* **17**, 1391–1401. <https://doi.org/10.1038/nm.2507> (2011).
8. Oliveira, T. H. C., Marques, P. E., Proost, P. & Teixeira, M. M. Neutrophils: a cornerstone of liver ischemia and reperfusion injury. *Lab. Invest.* **98**, 51–62. <https://doi.org/10.1038/labinvest.2017.90> (2018).
9. Jaeschke, H. & Lemasters, J. J. Apoptosis versus oncotic necrosis in hepatic ischemia/reperfusion injury. *Gastroenterology* **125**, 1246–1257. [https://doi.org/10.1016/s0016-5085\(03\)01209-5](https://doi.org/10.1016/s0016-5085(03)01209-5) (2003).
10. Weber, C., Fraemohs, L. & Dejana, E. The role of junctional adhesion molecules in vascular inflammation. *Nat. Rev. Immunol.* **7**, 467–477. <https://doi.org/10.1038/nri2096> (2007).
11. Martin-Padura, I. *et al.* Junctional adhesion molecule, a novel member of the immunoglobulin superfamily that distributes at intercellular junctions and modulates monocyte transmigration. *J. Cell. Biol.* **142**, 117–127. <https://doi.org/10.1083/jcb.142.1.117> (1998).
12. Nourshargh, S., Krombach, F. & Dejana, E. The role of JAM-A and PECAM-1 in modulating leukocyte infiltration in inflamed and ischemic tissues. *J. Leukoc. Biol.* **80**, 714–718. <https://doi.org/10.1189/jlb.1105645> (2006).
13. Khandoga, A. *et al.* Junctional adhesion molecule-A deficiency increases hepatic ischemia-reperfusion injury despite reduction of neutrophil transendothelial migration. *Blood* **106**, 725–733. <https://doi.org/10.1182/blood-2004-11-4416> (2005).
14. Del Maschio, A. *et al.* Leukocyte recruitment in the cerebrospinal fluid of mice with experimental meningitis is inhibited by an antibody to junctional adhesion molecule (JAM). *J. Exp. Med.* **190**, 1351–1356. <https://doi.org/10.1084/jem.190.9.1351> (1999).
15. Jaeger, B. N. *et al.* Neutrophil depletion impairs natural killer cell maturation, function, and homeostasis. *J. Exp. Med.* **209**, 565–580. <https://doi.org/10.1084/jem.20111908> (2012).
16. Hintermann, E. *et al.* Murine junctional adhesion molecules JAM-B and JAM-C mediate endothelial and stellate cell interactions during hepatic fibrosis. *Cell. Adhes. Migr.* **10**, 419–433. <https://doi.org/10.1080/19336918.2016.1178448> (2016).
17. Ostermann, G., Weber, K. S., Zerneck, A., Schroder, A. & Weber, C. JAM-1 is a ligand of the beta(2) integrin LFA-1 involved in transendothelial migration of leukocytes. *Nat. Immunol.* **3**, 151–158. <https://doi.org/10.1038/ni755> (2002).
18. Suzuki, S., Toledo-Pereyra, L. H., Rodriguez, F. J. & Cejalvo, D. Neutrophil infiltration as an important factor in liver ischemia and reperfusion injury. Modulating effects of FK506 and cyclosporine. *Transplantation* **55**, 1265–1272. <https://doi.org/10.1097/00007890-199306000-00011> (2006).
19. Zhang, Y. *et al.* Cholecystokinin protects mouse liver against ischemia and reperfusion injury. *Int. Immunopharmacol.* **48**, 180–186. <https://doi.org/10.1016/j.intimp.2017.03.028> (2017).
20. Lentsch, A. B., Kato, A., Yoshidome, H., McMasters, K. M. & Edwards, M. J. Inflammatory mechanisms and therapeutic strategies for warm hepatic ischemia/reperfusion injury. *Hepatology* **32**, 169–173. <https://doi.org/10.1053/jhep.2000.9323> (2000).
21. Ley, K., Laudanna, C., Cybulsky, M. I. & Nourshargh, S. Getting to the site of inflammation: The leukocyte adhesion cascade updated. *Nat. Rev. Immunol.* **7**, 678–689. <https://doi.org/10.1038/nri2156> (2007).
22. Jaeschke, H. & Farhood, A. Neutrophil and Kupffer cell-induced oxidant stress and ischemia-reperfusion injury in rat liver. *Am. J. Physiol.* **260**, G355–362. <https://doi.org/10.1152/ajpgi.1991.260.3.G355> (1991).
23. Zhai, Y., Busuttill, R. W. & Kupiec-Weglinski, J. W. Liver ischemia and reperfusion injury: New insights into mechanisms of innate-adaptive immune-mediated tissue inflammation. *Am. J. Transplant.* **11**, 1563–1569. <https://doi.org/10.1111/j.1600-6143.2011.03579.x> (2011).
24. Schwabe, R. F. & Brenner, D. A. Mechanisms of Liver Injury. I. TNF-alpha-induced liver injury: Role of IKK, JNK, and ROS pathways. *Am. J. Physiol. Gastrointest. Liver Physiol.* **290**, G583–589. <https://doi.org/10.1152/ajpgi.00422.2005> (2006).
25. Garrido-Urbani, S., Bradfield, P. F. & Imhof, B. A. Tight junction dynamics: The role of junctional adhesion molecules (JAMs). *Cell Tissue Res.* **355**, 701–715. <https://doi.org/10.1007/s00441-014-1820-1> (2014).
26. Giambelluca, M. S. *et al.* TNF-alpha expression in neutrophils and its regulation by glycogen synthase kinase-3: A potentiating role for lithium. *FASEB J.* **28**, 3679–3690. <https://doi.org/10.1096/fj.14-251900> (2014).
27. Colletti, L. M. *et al.* Role of tumor necrosis factor-alpha in the pathophysiologic alterations after hepatic ischemia/reperfusion injury in the rat. *J. Clin. Investig.* **85**, 1936–1943. <https://doi.org/10.1172/JCI114656> (1990).
28. Song, Z. *et al.* Exogenous melatonin protects small-for-size liver grafts by promoting monocyte infiltration and releases interleukin-6. *J. Pineal Res.* **65**, e12486. <https://doi.org/10.1111/jpi.12486> (2018).
29. Maas, S. L., Soehnlein, O. & Viola, J. R. Organ-specific mechanisms of transendothelial neutrophil migration in the lung, liver, kidney, and aorta. *Front. Immunol.* **9**, 2739. <https://doi.org/10.3389/fimmu.2018.02739> (2018).
30. Woodfin, A. *et al.* The junctional adhesion molecule JAM-C regulates polarized transendothelial migration of neutrophils in vivo. *Nat. Immunol.* **12**, 761–769. <https://doi.org/10.1038/ni.2062> (2011).
31. Cho, W. *et al.* Fate of neutrophils during the recovery phase of ischemia/reperfusion induced acute kidney injury. *J. Korean Med. Sci.* **32**, 1616–1625. <https://doi.org/10.3346/jkms.2017.32.10.1616> (2017).
32. Fukuhara, T. *et al.* A novel immunotoxin reveals a new role for CD321 in endothelial cells. *PLoS ONE* **12**, e0181502. <https://doi.org/10.1371/journal.pone.0181502> (2017).
33. Stamatovic, S. M., Sladojevic, N., Keep, R. F. & Andjelkovic, A. V. Relocalization of junctional adhesion molecule A during inflammatory stimulation of brain endothelial cells. *Mol. Cell. Biol.* **32**, 3414–3427. <https://doi.org/10.1128/MCB.06678-11> (2012).
34. Corada, M. *et al.* Junctional adhesion molecule-A-deficient polymorphonuclear cells show reduced diapedesis in peritonitis and heart ischemia-reperfusion injury. *Proc. Natl. Acad. Sci. USA* **102**, 10634–10639. <https://doi.org/10.1073/pnas.0500147102> (2005).
35. Liu, M. L. *et al.* Anti-inflammatory peptides from cardiac progenitors ameliorate dysfunction after myocardial infarction. *J. Am. Heart Assoc.* **3**, e001101. <https://doi.org/10.1161/JAHA.114.001101> (2014).
36. Lechner, F. *et al.* Antibodies to the junctional adhesion molecule cause disruption of endothelial cells and do not prevent leukocyte influx into the meninges after viral or bacterial infection. *J. Infect. Dis.* **182**, 978–982. <https://doi.org/10.1086/315765> (2000).
37. Kelly, J. M. *et al.* Induction of tumor-specific T cell memory by NK cell-mediated tumor rejection. *Nat. Immunol.* **3**, 83–90. <https://doi.org/10.1038/ni746> (2002).
38. Abe, Y. *et al.* Mouse model of liver ischemia and reperfusion injury: Method for studying reactive oxygen and nitrogen metabolites in vivo. *Free Radic. Biol. Med.* **46**, 1–7. <https://doi.org/10.1016/j.freeradbiomed.2008.09.029> (2009).
39. Panel, M. *et al.* Small-molecule inhibitors of cyclophilins block opening of the mitochondrial permeability transition pore and protect mice from hepatic ischemia/reperfusion injury. *Gastroenterology* **157**, 1368–1382. <https://doi.org/10.1053/j.gastro.2019.07.026> (2019).
40. Wang, X. *et al.* Dusp14 protects against hepatic ischaemia-reperfusion injury via Tak1 suppression. *J. Hepatol.* <https://doi.org/10.1016/j.jhep.2017.08.032> (2017).
41. Hu, J. *et al.* Targeting TRAF3 signaling protects against hepatic ischemia/reperfusion injury. *J. Hepatol.* **64**, 146–159. <https://doi.org/10.1016/j.jhep.2015.08.021> (2016).
42. Ocuin, L. M. *et al.* Nilotinib protects the murine liver from ischemia/reperfusion injury. *J. Hepatol.* **57**, 766–773. <https://doi.org/10.1016/j.jhep.2012.05.012> (2012).
43. Yin, E., Matsuyama, S., Uchiyama, M., Kawai, K. & Niimi, M. Graft protective effect and induction of CD4(+)Foxp3(+) cell by Thrombomodulin on allograft arteriosclerosis in mice. *J. Cardiothorac. Surg.* **13**, 48. <https://doi.org/10.1186/s13019-018-0731-8> (2018).

44. Kojima, Y., Nishina, T., Nakano, H., Okumura, K. & Takeda, K. Inhibition of importin beta1 augments the anticancer effect of agonistic anti-death receptor 5 antibody in TRAIL-resistant tumor cells. *Mol. Cancer Ther.* **19**, 1123–1133. <https://doi.org/10.1158/1535-7163.MCT-19-0597> (2020).
45. Martino, T. A. *et al.* Circadian rhythm disorganization produces profound cardiovascular and renal disease in hamsters. *Am. J. Physiol. Regul. Integr. Comp. Physiol.* **294**, R1675–1683. <https://doi.org/10.1152/ajpregu.00829.2007> (2008).
46. Takahashi, M. *et al.* The phytosphingosine-CD300b interaction promotes zymosan-induced, nitric oxide-dependent neutrophil recruitment. *Sci. Signal.* <https://doi.org/10.1126/scisignal.aar5514> (2019).
47. Takeda, K. *et al.* Involvement of tumor necrosis factor-related apoptosis-inducing ligand in surveillance of tumor metastasis by liver natural killer cells. *Nat. Med.* **7**, 94–100. <https://doi.org/10.1038/83416> (2001).

Acknowledgements

We thank Laboratory of Morphology and Image Analysis, Research Support Center, Juntendo University Graduate School of Medicine for technical assistance with histopathology and immunohistochemistry study. This study was partly supported by KAKENHI, a Grant-in-Aid for Scientific Research C (T.F.: 16K07184, 19K07831).

Author contributions

E.Y. participated in writing the manuscript, data analysis, and performance of the research. T.F. and K.T. participated in research design, writing the manuscript, and data analysis. Y.K. participated in performance of the research. K.F., K.I., and H.B. participated in data analysis. H.Y. and K.O. participated in research design. K.U. participated in research design, oversaw the study, and data analysis. All authors reviewed the manuscript.

Competing interests

The authors declare no competing interests.

Additional information

Supplementary Information The online version contains supplementary material available at <https://doi.org/10.1038/s41598-021-85001-2>.

Correspondence and requests for materials should be addressed to T.F. or K.U.

Reprints and permissions information is available at www.nature.com/reprints.

Publisher's note Springer Nature remains neutral with regard to jurisdictional claims in published maps and institutional affiliations.



Open Access This article is licensed under a Creative Commons Attribution 4.0 International License, which permits use, sharing, adaptation, distribution and reproduction in any medium or format, as long as you give appropriate credit to the original author(s) and the source, provide a link to the Creative Commons licence, and indicate if changes were made. The images or other third party material in this article are included in the article's Creative Commons licence, unless indicated otherwise in a credit line to the material. If material is not included in the article's Creative Commons licence and your intended use is not permitted by statutory regulation or exceeds the permitted use, you will need to obtain permission directly from the copyright holder. To view a copy of this licence, visit <http://creativecommons.org/licenses/by/4.0/>.

© The Author(s) 2021